Bioactive Materials 24 (2023) 322–330

Contents lists available at ScienceDirect

Bioactive Materials

journal homepage: www.keaipublishing.com/en/journals/bioactive-materials

Copper-cysteamine nanoparticle-mediated microwave dynamic therapy improves cancer treatment with induction of ferroptosis

Hui Zhou [a,1], Zhongtao Liu [a,1], Zijian Zhang [a], Nil Kanatha Pandey [b], Eric Amador [b], William Nguyen [b], Lalit Chudal [b], Li Xiong [a,***], Wei Chen [b,**], Yu Wen [a,*]

[a] Department of General Surgery, Second Xiangya Hospital, Central South University, Changsha, 410011, China
[b] Department of Physics, The University of Texas at Arlington, Arlington, TX, 76019-0059, USA

ARTICLE INFO

Keywords:
Cu-Cy
Microwave
PDT
Cell death
Colorectal cancer
Ferroptosis

ABSTRACT

Photodynamic Therapy (PDT) holds a great promise for cancer patients, however, due to the hypoxic characteristics of most solid tumors and the limited penetration depth of light in tissues, the extensive clinical application of PDT is limited. Herein, we report microwave induced copper-cysteamine (Cu-Cy) nanoparticles-based PDT as a promising cancer treatment to overcome cancer resistance in combination with ferroptosis. The treatment efficiency of Cu-Cy-mediated microwave dynamic therapy (MWDT) tested on HCT15 colorectal cancer (CRC) cells via cell titer-blue cell viability assay and live/dead assay reveal that Cu-Cy upon MW irradiation can effectively destroy HCT15 CRC cells with average IC-50 values of 20 μg/mL. The cytotoxicity of Cu-Cy to tumor cells after MW stimulation can be alleviated by ferroptosis inhibitor. Furthermore, Cu-Cy mediated MWDT could deplete glutathione peroxide 4 (GPX4) and enhance lipid peroxides (LPO) and malondialdehyde (MDA). Our findings demonstrate that MW-activated Cu-Cy killed CRC cells by inducing ferroptosis. The superior *in vivo* antitumor efficacy of the Cu-Cy was corroborated by a HCT15 tumor-bearing mice model. Immunohistochemical experiments showed that the GPX4 expression level in Cu-Cy + MW group was significantly lower than that in other groups. Overall, these findings demonstrate that Cu-Cy nanoparticles have a safe and promising clinical application prospect in MWDT for deep-seated tumors and effectively inhibit tumor cell proliferation by inducing ferroptosis, which provides a potential solution for cancer resistance.

1. Introduction

Cancer is a major public health problem worldwide, with few effective treatment [1]. The main antitumor treatment options are chemotherapy and radiation therapy. However, acquired resistance has created a serious challenge for anticancer treatments. The exact mechanism of drug resistance is complex, but can be classified into three groups: insufficiency of pharmacokinetic properties, intrinsic factors of tumor cells, and external conditions of tumor cells in tumor microenvironment (TME) [2]. Several studies have shown that the TME promotes cancer progression in various ways, especially therapeutic resistance [3]. The TME reduces the penetration of drug and confer the advantage of proliferation and anti-apoptosis to surviving cells, facilitating resistance, and modifying disease morphology. Hypoxia is a typical feature in nearly all solid tumors, due to uncontrolled cell proliferation, abnormal tumor vessels, and insufficient oxygen supply, which is closely linked with resistance to chemotherapy and PDT [4,5]. A simple and commonly recognized reason that hypoxia can negatively affect the treatment efficiency is large reduction in the ROS production in the hypoxic condition. Therefore, exploring nanomaterials that can generate a large amount of ROS in response to the TME is an emerging strategy for cancer therapy [6].

TME greatly affects the efficacy of nanomaterials, one exception are Cu(I)-based nanoparticles which are more versatile in weakly acidic environments and actually give high ·OH yield [7]. The reaction rate of Cu(I) based Fenton reaction is much greater than that of Fe-based Fenton

Peer review under responsibility of KeAi Communications Co., Ltd.
* Corresponding author.
** Corresponding author.
*** Correponding author
E-mail addresses: lixionghn@csu.edu.cn (L. Xiong), weichen@uta.edu (W. Chen), wenyu2861@csu.edu.cn (Y. Wen).
[1] Contributed equally.

https://doi.org/10.1016/j.bioactmat.2022.12.023
Received 29 October 2022; Received in revised form 18 December 2022; Accepted 22 December 2022

reaction [8]. Furthermore, the excess glutathione (GSH) in the TME could reduce the Cu(II) produced by Fenton-like reaction to Cu(I), which further accelerates the reaction rate [9]. All these can be evidenced in our recent publication on copper-cysteamine (Cu-Cy) nanoparticles-based Fenton-like therapy on cancer treatment [10]. Moreover, Fenton and Fenton-like reactions could be enhanced by increasing the temperature above 35 ^{o}C in the presence of Cu(I)-based nanomaterials and may show a significant enhancement over Fe-based nanoparticles [11].

Common PDT through type II mechanism relies on singlet oxygen ($^1O_2$) generated by photosensitizers upon light irradiation, leading to tumor cell necrosis or apoptosis [12]. However, therapeutic efficacy of type II-PDT is severely hampered by inadequate oxygen levels [13]. Fortunately, microwave-induced PDT is a good substitute for type-I based PDT. MW refers to the electromagnetic wave of 900–2450 MHz, which is widely used in clinical tumor ablation [14]. Compared with traditional surgical resection, MW ablation has certain advantages, including shorter treatment time, safety and accuracy, pinhole size, rapid healing, no scarring, lower surgical mortality, and increased protection of surrounding soft tissues [15]. Furthermore, MW has a deeper penetration than most light, including NIR. Microwave dynamic therapy (MWDT) is a new method for tumor therapy, which could overcome the limitation of insufficient penetration depth of traditional PDT [16–18]. Additionally, MW can produce a thermal effect in the process of exciting the photosensitizer that can improve the treating efficacy. Tissue is heated by MW irradiation, which leads to blood vessel dilation and thus accelerates blood flow, allowing for elevated oxygen levels and increased therapeutic effect [19]. MWDT is a typical type-I based PDT as microwave cannot excite the photosensitizers to trigger luminescence and/or energy transfer for type-II based PDT.

Recently, a new type of programmed cell death called ferroptosis, has gradually been recognized by researchers, and the concept of ferroptosis induced by PDT has gradually been proposed [20]. In short, ferroptosis is a process in which ferrous ions (Fe^{2+}) catalyze ROS to oxidize polyunsaturated fatty acids to form lipid peroxides. Fe^{2+} and ROS are considered to be necessary factors for ferroptosis [21]. Therefore, the ROS produced by PDT may cause higher levels of ferroptosis in the presence of Fe^{2+}, thereby avoiding cell resistance to apoptosis. In particular, cancer cells that are resistant to conventional therapies or have a high propensity for metastasis may be particularly susceptible to ferroptosis, so inducing ferroptosis in cancer cells is a promising therapeutic modality [22]. In addition, previous studies have shown that ferroptosis is associated with cancer treatment resistance and can even reverse the therapeutic role of cancer in resistance to common therapies such as chemotherapy, targeted therapy, and immunotherapy [23]. The curcumin analogue inhibits GPX4, thereby inducing ferroptosis and overcoming temozolomide resistance [24]. A previous study demonstrated sulfasalazine inhibits Solute carrier family 7 member 11 (SLC7A11)-induced ferroptosis and overcomes olaparib resistance [25]. In addition, resistance to anti-programmed cell death 1 (PD-1)/programmed death ligand 1 (PD-L1) therapy may be caused by inhibition of ferroptosis [26].

Cu-Cy nanoparticle, as a novel generation of sensitizer, can be irradiated by ultraviolet light [27–30], ultrasound [31], X-rays [32–34] and MWs [35,36] to produce highly toxic ROS for cancer cell destruction. Furthermore, Cu-Cy nanoparticles can kill both gram-positive and gram-negative bacteria under ultraviolet light when combined with potassium iodide (KI) [29]. Cu-Cy nanoparticles can also act as a heterogeneous Fenton-like catalyst for selective cancer killing [10]. Our recent work has showed that Cu-Cy nanoparticles can enhance the anticancer effect of disulfiram, an FDA-approved drug, on esophageal cancer [37]. Cu-Cy poses several advantages, including long half-life, low cytotoxicity, higher $^1O_2$, lower cost, and is easier to synthesize [27].

In this work, we found that microwave PDT based on Cu-Cy nanoparticles can effectively stimulate iron drop. Our results suggest that Cu-Cy-mediated MWDT may provide a new option for the clinical treatment of colorectal cancer (CRC), one of the three major malignant tumors with a high incidence. It also makes up for the lack of tissue penetration depth in PDT treatment. In addition, microwave heating is a good solution to increase oxygenation to overcome hypoxia for PDT outcomes. All these results suggest a potential therapeutic approach for drug-resistant and radiation-resistant cancers.

2. Materials and methods

2.1. Synthesis and characterization of Cu-Cy nanoparticles

Cu-Cy nanoparticles were fabricated as discussed in our previous publications [28,35]. The absorption spectra were monitored using a UV–Vis spectrophotometer (Shimadzu UV-2450, Japan) and the photoluminescence emission and excitation spectra were collected using a Spectro-fluorophotometer (Shimadzu RF-5301PC, Japan).

2.2. Cell culture

HCT15 cell line was obtained from Cell Resource Center, Chinese Academy of Medical Science (Shanghai, China). HCT15 cells were incubated in RPMI 1640 (GIBCO, USA) culture media (5% CO_2) that was supplemented with 10% fetal bovine serum (FBS, GIBCO, USA) and 1% penicillin-streptomycin. The temperature was kept at 37 °C in an incubator.

2.3. The use of microwave system

MW was delivered to the cell via a radiator probe with a frequency of 2450 MHz. The MW was generated by the WB-3100AI medical MW generator (Xuzhou Baoxing Medical Equipment Co., LTD., China).

2.4. RNO-ID assay

ROS produced by Cu-Cy nanoparticles under MW irradiation was detected by p-nitrosodimethylaniline (RNO) (Sigma, USA) and imidazole (ID) (Sigma, USA) method. Briefly, 0.225 mg of RNO and 16.34 mg of ID were dissolved in 30 mL of DI water separately. These solutions were experimentally saturated with enough bubble air. Sample solution was prepared by mixing 1 mL of RNO, 1 mL of ID, and 1 mL of 200 μg/mL Cu-Cy aqueous solution. Then, a spectrophotometer (Thermo Fisher Scientific,MA,USA) was used to measure the absorption intensity of RNO. The controlled experiment was conducted following the same steps, except deionized water was used instead of Cu-Cy nanoparticles.

2.5. Detection of singlet oxygen ($^1O_2$) by singlet oxygen sensor green (SOSG) fluorescent probe

A singlet oxygen sensor green reagent (SOSG) (Ex = 505 nm, Em = 525 nm) was used to detect the $^1O_2$ in the aqueous solution. SOSG (100 μg, Meilunbio, China) was dissolved in methanol (33 μL) to make a 5 mM stock solution. The SOSG stock solution was diluted with PBS to a working solution of 50 μM. 100 μL of Cu-Cy nanoparticles (10, 20, 40, and 80 μg/mL) were loaded into four wells of a 96-well plate, and 10 μL of SOSG stock solution was added to each well. After mixing, MW (20 W, 3 min) was irradiated, and the fluorescence of SOSG was measured with a microplate reader immediately after each microwave treatment.

2.6. Live/dead assay

We further evaluated the cell viability upon MW irradiation by using a live/dead cell viability assay (Beyotime, China). 5×10^5 cells/well were implanted into a 6-well plate and incubated in a cell incubator for 24 h at 37 °C in a humidified atmosphere of 5% CO_2. Following the incubation, the old media was removed, and 2 mL of fresh media with or without 20 μg/mL of Cu-Cy was added to each well. The experiment

consisted of four groups: control (cell only), MW, Cu-Cy, Cu-Cy + MW. The cells were incubated with Cu-Cy for 24 h in the incubator, and then the MW group and the Cu-Cy + MW group were subjected to irradiation with MW (2450 MHz, 20 W, 3 min) through the radiator probe. The treated cells were placed in the incubator for another 24 h, and the old media was replaced with 500 μL fresh media containing calcein-AM and propidium iodide (PI) mixture. The cells were incubated for another 45 min under dark conditions at 37 °C. Finally, the stained cells were observed under a fluorescence microscope.

2.7. Cell titer blue cell activity assay

5×10^5 cells/well were implanted into a 6-well plate. After incubation at 37 °C for 24 h, fresh culture media with or without Cu-Cy was added respectively. After incubating for 24 h in an incubator, the MW treatment was carried out. Cell viability was determined using Cell TiTER-Blue® kit (Promega Co.Ltd). Briefly, 200 μL of Cell Titer-Blue reagent was added to each well and cultured in an incubator for 2 h. Fluorescence at 560/590 nm was determined using a microplate reader. The cell viability of experimental samples was calculated by comparing their fluorescence intensities with that of the control group. Three different iron death inhibitors, 5 mM N-Acetylcysteine (NAC), 100 μM deferoxamine (DFO), and 1 μM ferrostatin-1 (Fer-1) were used to investigate the effect of ferroptosis inhibition on Cu-Cy (20 μg/mL) mediated MWDT.

2.8. Colony formation assay

To study colony formation, HCT15 cells (1000 cells/well) were seeded in six-well plates overnight to allow cells to attach to the plate surface. The cells were incubated with Cu-Cy (20 μg/mL) for 24 h and then treated with MW. Colony formation was assessed after 10 days of the treatment. Colonies were fixed with 4% paraformaldehyde and stained with 0.05% methylene blue.

2.9. Malondialdehyde (MDA) assay

The relative MDA concentration in cell lysates of control and experimental groups were evaluated using a lipid peroxidation assay kit (S0131S, Beyotime) according to the manufacturer's instructions. Briefly, 3 h after microwave treatment, cells were lysed in lysate, incubated with MDA detection working solution at 100 °C for 15 min, centrifuged, and then 200 μL of supernatant was added to a 96-well plate. Subsequently, absorbance was measured at 532 nm using a microplate reader.

2.10. BODIPY 581/591 C11 analysis

HCT15 cells were evenly seeded in 6-well plates at 5×10^5 cells/well. When the cell density reached about 80%, the Cu-Cy dispersed in complete media (0 and 20 μg/mL, in 2 mL) was added to the 6-well plate and incubated in dark for 24 h. Next, 3 h after microwave treatment, the original media was aspirated, washed twice with PBS, and incubated with 1 mL of media containing 10 μmol/L BODIPY^{TM} 581/591 C11 (D3861, Thermo-fisher Scientific, MA,USA) at 37 °C for 30 min in a cell incubator. The plate was wrapped with aluminum foil to protect the cells from light to avoid unnecessary photoactivation. To remove the excess dye, the cells were washed three times with PBS, then trypsinized and resuspended in PBS. Using a flow cytometer (NL-3000,Cytek), the cells were excited with lasers at 488 nm and 565 nm, and the corresponding signals at 505 nm–550 nm were measured in the FL1 channel, and the signals above 580 nm were measured in the FL2 channel. Finally, the results were analyzed using FlowJo 10.6 software.

2.11. Western blot

Cell protein was extracted 6 h after microwave treatment. Total protein was extracted with cell lysis buffer containing a mixture of protease and phosphatase inhibitors (50 mM Tris, 150 mM NaCl, 1% NP-40, 1 mM EDTA, pH 7.6). Protein concentration was determined using the BCA protein assay kit. The sample (30 μg protein/swimlane) was isolated by SDS-PAGE and transferred to the PVDF membrane. After sealing with TBST buffer containing 5% skimmed milk (20 mM Tris, 137 mM NaCl, 0.1% Tween-20, pH8.0), the membrane was incubated with primary antibodies such as GPX4 (1:1000) and GAPDH (1:1000) at 4 °C overnight. The membrane was then incubated with a secondary antibody (1:2000) at room temperature for 1 h and washed 3 times with 0.3% Tween 20-TBS. Protein bands were visualized using Immobilon Western chemiluminescent HRP substrates.

2.12. In vivo xenograft mouse study

The following animal work was approved by the Animal Ethics Committee of Second Xiangya Hospital (Changsha, China). Five-week-old female athymic BALB/c nude mice were randomly divided into four groups: 1) control, 2) MW, 3) Cu-Cy, and 4) Cu-Cy + MW. The cells (5×10^6) in a volume of 200 μL were inoculated into the subcutaneous tissue of the left flank of nude mice; four animals were used per group. Treatment was undertaken when the tumor size (length) reached 5–8 mm. Mice were anesthetized using isoflurane gas. For Cu-Cy group, Cu-Cy nanoparticles were injected in 30 μL of PBS at a concentration of 1 μg/μL. For MW treatment, the MW was delivered directly to the tumors through a radiator probe after 24 h post-injection. The tumor size and body weight were measured daily. The tumor volume was calculated using the formula: tumor volume = (width^2 × length)/2. HCT15 tumor-bearing mice were treated with three injections of Cu-Cy on 0, 3rd, 6th, and 9th day. MW irradiation was performed on 1st, 4th, 7th, and 10th day. All mice were euthanized, and tumors were harvested on the 10th day; the specimen was fixed in buffered neutral formalin. Subsequently, the sections were fixed by formaldehyde and embedded in paraffin for histological analysis. The sections were stained with hematoxylin and GPX4 and observed under microscope.

2.13. Statistical analysis

All quantitative data were expressed as mean ± SD and were performed at least three times. One-way analysis of variance (ANOVA) and the unpaired Student's t-test were used to determine whether there was statistical significance between the control group and the experimental group using GraphPad Prism 9.0. *$p < 0.05$, **$p < 0.01$, ***$p < 0.001$ and ****$P < 0.0001$ were considered statistically significant.

3. Results

3.1. Characterization of Cu-Cy nanoparticles

The detailed synthesis procedure, characterizations, and crystal-structure of Cu-Cy nanoparticles were discussed in our previous publications [28,35]. Fig. 1A displays the UV–vis absorption curve of the Cu-Cy nanoparticles in DI water, with an absorption peak at ~365 nm. The photoluminescence emission spectrum (red) under 365 nm excitation and excitation curve (blue) upon 607 nm emission of Cu-Cy nanoparticles are shown in Fig. 1B. Cu-Cy nanoparticles exhibit intense photoluminescence when excited by ultraviolet light. The inset of Fig. 1B displays the photographs of the Cu-Cy nanoparticles in DI water under ambient light (right) and ultraviolet light (left).

3.2. Detection of ROS production

The ROS production from Cu-Cy upon MW irradiation were assessed

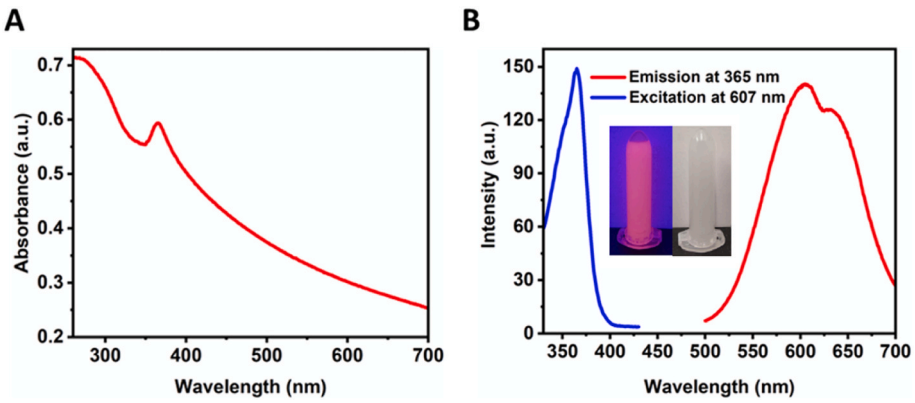

Fig. 1. (A) UV–vis absorption curve of Cu-Cy nanoparticles in DI water. (B) The spectra of excitation (left, blue) at 607 nm and emission (right, red) at 365 nm of the Cu-Cy suspended in DI water. Inset: Images of the Cu-Cy at 1 mg/ml in DI water under UV light (left) and at ambient light (right).

using RNO-ID and SOSG. We also note that the absorption of RNO is quenched with increasing MW power, as indicated in Fig. 2A. This means that as the MW irradiation power is increased, the ROS increases as well, in accordance with our previous studies [35,38–40]. Fig. 2B shows the ROS produced by Cu-Cy nanoparticles at various time points under 20 W of microwave radiation. Absorption of RNO quenched with the increase of MW time, which means as the MW irradiation time is increased there is more ROS. The fluorescence of SOSG is continuously enhanced, with the increase of Cu-Cy concentration, which indicates that the singlet oxygen is continuously increased (Fig. 2C).

3.3. MW activated Cu-Cy inhibited the proliferation of human CRC cells

The toxicity of Cu-Cy nanoparticles was evaluated by cell titer blue cell viability assay after the nanoparticles were cultured with HCT15 cells for 24 h. As shown in Fig. 3A, the cell viability gradually decreased from 99% to 84% when the Cu-Cy concentration increased from 10 μg/mL to 40 μg/mL. As a primary conclusion, the Cu-Cy nanoparticles have low toxicity at these concentrations. Under the MW irradiation with different concentrations of Cu-Cy, the cell viability was concentration-dependent, and the higher the concentration, the more obvious the killing effect (Fig. 3A). Cu-Cy doses of 20 μg/mL with MW irradiation (20 W, 3 min) resulted in cell growth inhibition rates of 56%. Therefore, 20 μg/mL was used as the experimental concentration for *in vitro* experiments. To further evaluate the effect of the Cu-Cy mediated MWDT on CRC cell, cell proliferation was examined by live/dead assay. As shown in Fig. 3B, when Cu-Cy was activated by 3 min of MW (20 W), the cytotoxicity was significantly enhanced when compared to their corresponding controls (Cu-Cy alone). With the increase of Cu-Cy concentration, the cytotoxic effect of MWDT became stronger and stronger. Especially when the concentration of Cu-Cy reached 40 μg/mL, almost all cells were dead after microwave excitation. When the concentration of Cu-Cy was 20 μg/mL, about half of the cells died after MW excitation. To evaluate the long-term antiproliferative effect, we performed a colony formation assay using a Cu-Cy concentration of 20 μg/mL. The results of the colony formation assay (Fig. 3C and D) show that MW

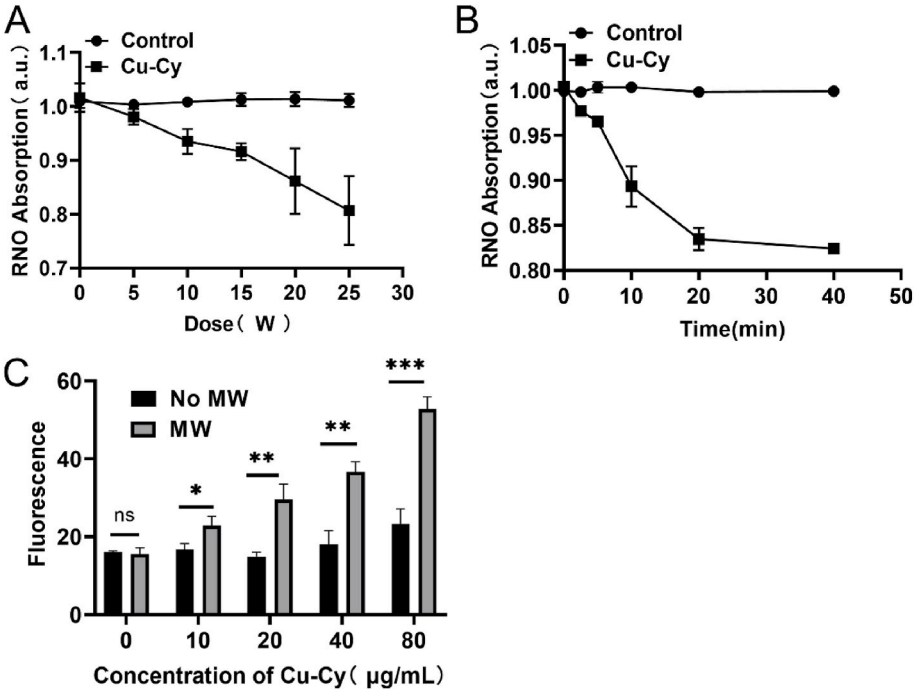

Fig. 2. Detection of ROS in aqueous solution. (A) RNO-ID method was used to detect ROS produced by Cu-Cy aqueous solution (0.2 mg/ml) irradiated by MW of different power for 5 min. (B) RNO-ID method was used to detect ROS produced by Cu-Cy aqueous solution (0.2 mg/ml) irradiated with MW at 20 W for different time. (C) Fluorescence intensity of SOSG with the different Cu-Cy concentrations after MW irradiation. *P < 0.05, **P < 0.01, ***P < 0.001.

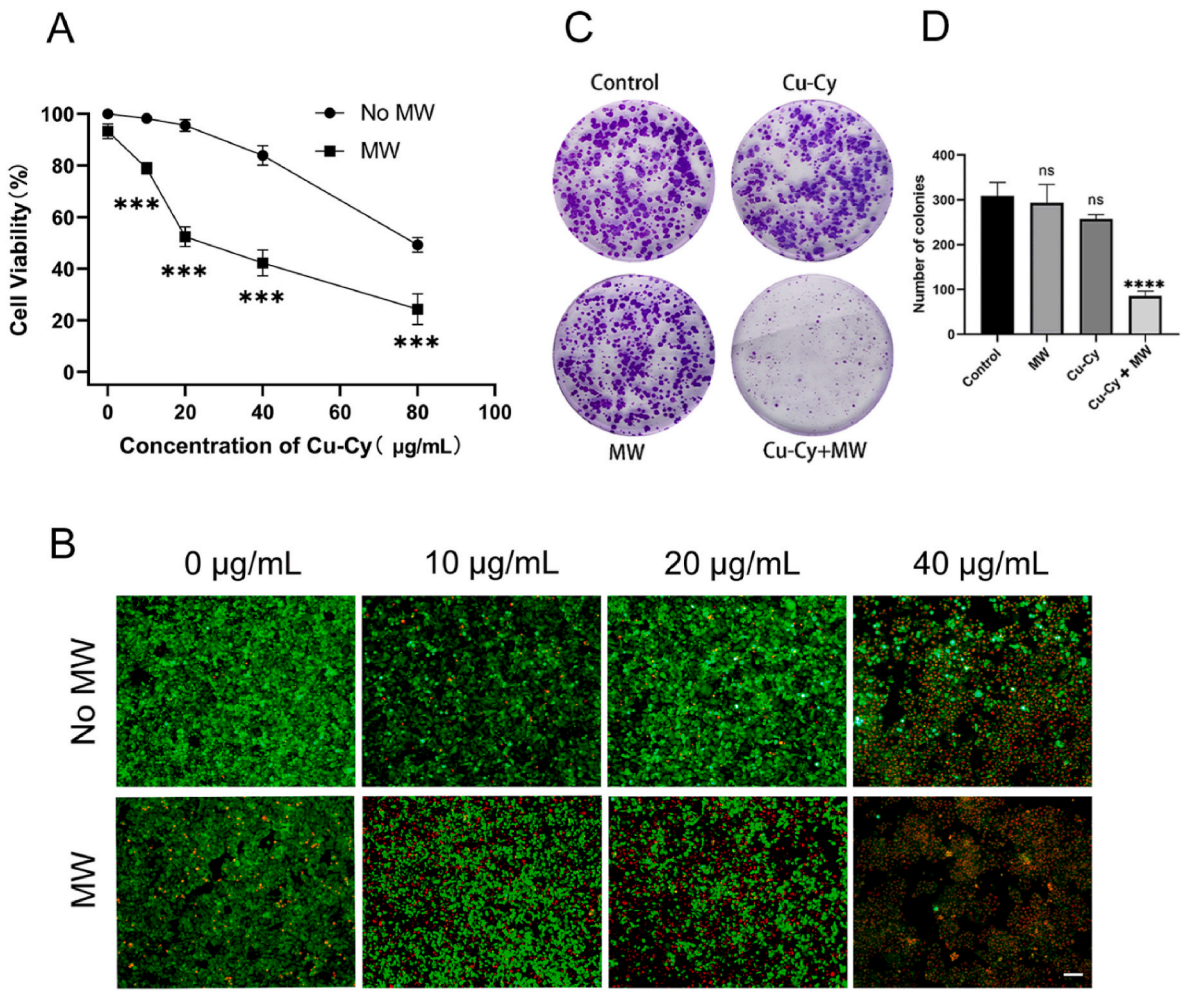

Fig. 3. *In vitro* cell study of MWDT. (A) The cell viability of HCT15 cells was evaluated by cell titer blue cell viability assay after treating 0, 10, 20, 40, or 80 μg/mL of Cu-Cy nanoparticles with or without MW irradiation. (B) The live/dead staining images of HCT15 cells with Cu-Cy and MW irradiation (20 W, 3 min). (C) Colony formation study in HCT15 cells treated with MW. (D)The average number of clones was calculated. Scale bar: 50 μm ***P < 0.001 and ****P < 0.0001.

activated Cu-Cy nanoparticles significantly inhibited cell colony formation compared to other groups. However, there is no significant difference in the colony counts among Cu-Cy group, MW group, and control group. These results suggest that MW-activated Cu-Cy nanoparticles can inhibit the proliferation of human CRC cells HCT15.

3.4. *MW activated Cu-Cy nanoparticles induced the ferroptosis of human CRC cells*

Our previous studies have demonstrated that Cu-Cy-mediated PDT can trigger various forms of cell death, including apoptosis and autophagy [34,35]. To deeply investigate the antitumor effect of MWDT treatment, we further investigated whether MW activated Cu-Cy could induce ferroptosis cell death *in vitro*. In HCT-15 cell line, we first tested the rescue effect of typical ferroptosis inhibitors NAC, DFO, and Fer-1 after MWDT treatment. Surprisingly, these three ferroptosis inhibitors had a significant rescue effect (Fig. 4A). Accordingly, ferroptosis may be the main cell death pathway in MWDT treatment. To this end, we further detected the contents of GPX4, MDA and lipid peroxides (LPO). The expression of GPX4 was confirmed by the Western blot. As seen in Fig. 4B, the relative weak signal of the GPX4 band was presumed due to its low expression in HCT15 treated with MWDT compared to other groups. LPO inside cells was generally regarded as the hallmark of ferroptosis [41]. Using the fluorescent probe C11-BODIPY, we observed the lipid peroxidation was higher in the HCT15 cells treated with Cu-Cy + MW than in the cells treated with MW alone or Cu-Cy alone (Fig. 4C and D). The increased MDA in HCT15 cell was further confirmed by MDA assay (Fig. 4E). The results revealed elevated MDA content in the Cu-Cy + MW (11.8 μM/g) group when compared to control group (4.46 μM/g). The level of MDA in Cu-Cy (4.83 μM/g) and MW (4.24 μM/g) groups was similar to that in the control group. An additional group, Cu-Cy + MW + Fer-1 was included and compared with the other groups to observe the change in the expression of GPX4, MDA level, and LPO level. Consequently, the variation of expression of GPX4, activity of GPX4, MDA, and LPO caused by Cu-Cy + MW were all retained, which evidenced that ferroptosis is essential in the treatment. In summary, these findings suggested that MW activated Cu-Cy induced the ferroptosis of human CRC cells.

3.5. *MWDT significantly inhibited tumor growth in vivo*

We further investigated the role of the treatment efficiency of MWDT by means of xenograft nude mouse model. HCT15 cells were injected subcutaneously into the subcutaneous tissue of the left flank of nude mice to establish a tumor-bearing mice model (Fig. 5A). The xenograft nude mouse was randomly divided into four groups as indicated in Fig. 5B. There was a 10-day observation of tumor volumes and body weights of mice after MWDT to investigate the anti-tumor efficacy of combination therapy *in vivo*. MWDT treatment significantly inhibited the tumor growth (Fig. 5C and E). The tumor volume and weight in the

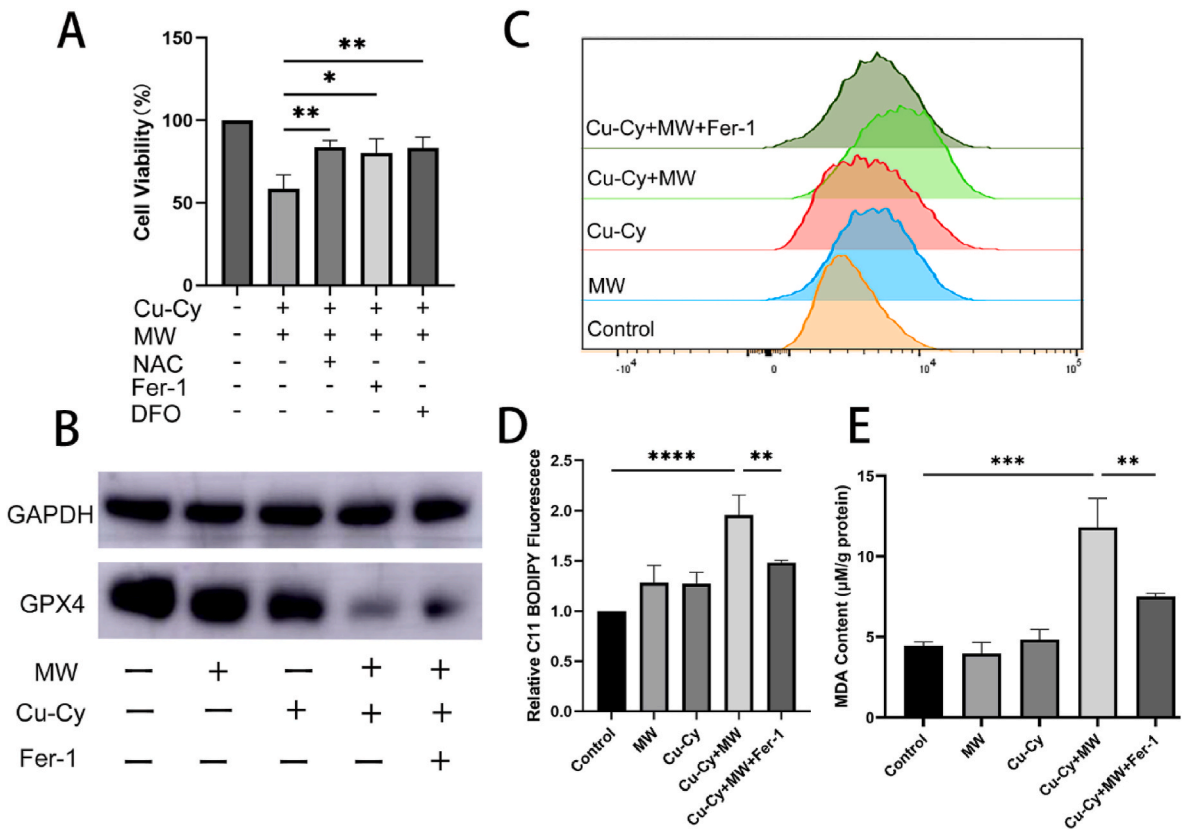

Fig. 4. Function of MWDT in ferroptosis induction. (A) Cell viability after treated with 5 mM of NAC, 100 μM of DFO, 1 μM of Fer-1, and 20 μg/mL of Cu-Cy under MW irradiation. (B) Western blot assay of GPX4 expression. (C) FCM assay of cellular LPO with BODIPY-C11 probe detection. (D) Relative fluorescence intensity of HCT15 stained by C11 BODIPY probe by FCM. (E) MDA examination under different treatments. *P < 0.05, **P < 0.01, ***P < 0.001,****P < 0.0001.

Cu-Cy + MW group were decreased compared to that of the control group (tumor volume: $p < 0.05$, tumor weight: $p < 0.05$, Fig. 5C and E). Moreover, there was no significant difference in body weight among the four groups (Fig. 5D). These results indicate that Cu-Cy has a good antitumor effect after MW excitation. In addition, the expression level of GPX4 in the Cu-Cy + MW group was significantly lower than that in the other groups, suggesting that ferroptosis may play a role in antitumor therapy (Fig. 5F and G).

4. Discussion

CRC is one of the three major malignant tumors and is the second leading cause of cancer related death [42]. In recent years, the incidence and mortality rates of CRC have been steadily increasing due to changes in lifestyle and diet. Due to the severe side effects and poor prognosis of existing clinical therapies, there is an urgent need for new effective treatments for advanced metastatic CRC. Moreover, adjuvant chemotherapy of CRC does not completely eliminate circulating tumor cells, even after surgical removal of the primary tumor [43]. Therefore, it is crucial to explore novel therapeutic strategies for CRC.

In recent years, PDT has become a widely accepted clinical treatment for malignant tumors. However, the hypoxic nature of solid tumors reduces its therapeutic effectiveness. In addition, the limited penetration depth of light also limits the wide clinical application of PDT. Here, we propose the concept of MWDT. MW has a deeper penetration depth than most light including NIR. Also, MW can produce thermal effect in the process of excitation of photosensitizer that can improve the treating efficacy. Tissue is heated by MW technology, which leads to blood vessel dilation and thus accelerates blood flow, allowing for elevated oxygen levels and increased therapeutic effect [19].

In our study, we used the RNO-ID method and SOSG assay to detect ROS. RNO absorption quenched continuously with the increase of MW power and time, which means more ROS was produced as the MW power and time increased. The intensity of green fluorescence signal produced by SOSG is related to the content of singlet oxygen. To investigate the antitumor efficiency of Cu-Cy nanoparticle mediated MWDT in CRC, we performed *in vitro* and *in vivo* experiments in HCT15 cells. The effect of Cu-Cy induced MWDT on HCT15 cell viability was verified by cell titer blue cell viability assay. The results showed that Cu-Cy induced by MW could significantly inhibit cell viability. The antitumor effect of Cu-Cy induced by MW was confirmed by the results of cell staining and clonogenesis. In addition, xenograft tumor model experiments showed similar results: tumor volume in the Cu-Cy + MW group was significantly reduced compared to the control group. No obvious signs of weight change were observed among the four groups of experiments, indicating that MW-induced Cu-Cy had no adverse effects on the growth of mice.

Cu-Cy can produce ROS by MW excitation, which means oxidative stress and ROS can cause DNA damage. It has been confirmed that MW stimulation of Cu-Cy can induce apoptosis of osteosarcoma cells [36]. Apoptosis is the main mechanism of tumor cell death induced by PDT. But in recent years, ferroptosis have also been found to be closely related to ROS. Ferroptosis is a non-apoptotic form of cell death driven by phospholipid peroxidation of iron-dependent polyunsaturated fatty acids, which is caused by oxidative damage [44]. Ferroptosis was first identified and named by Professor Brent R. Stockwell in 2012 [45]. Ferroptosis was closely associated with damage or degenerative diseases in a variety of organs, including the kidneys and brain, which is considered to be a potentially targeted pathway in a variety of cancers. Ferroptosis can be triggered externally or internally [46]. The external pathway is initiated by inhibiting cell membrane transporters such as cystine/glutamate transporters (also known as the XC-system) or by

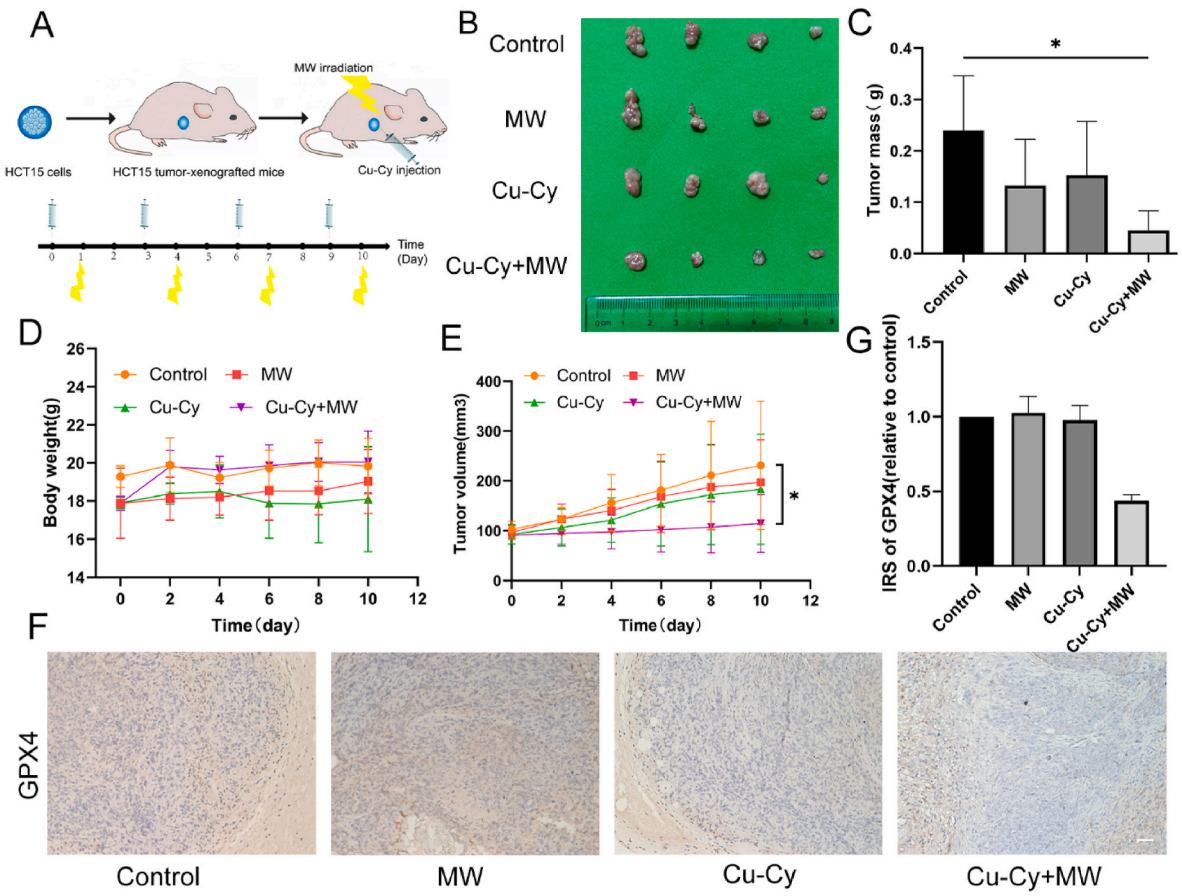

Fig. 5. Antitumor effect of MWDT in mouse subcutaneous tumor models. (A) A schematic diagram of MWDT scheme for animal experiments. HCT15 tumor-bearing mice were treated with three injections of Cu-Cy on 0^{th}, 3rd, 6th, and 9th day. MW irradiation was performed on 1st, 4th, 7th, and 10th day. The tumor size and body weight were measured daily. (B) Images of each group at the end of the xenograft model experiment. (C) Tumor mass changes. (D) Body weight changes. (E) Tumor volume changes. (F) Histological observation of the tumor tissues with GPX4 staining. Scale bar: 50 μm *p < 0.05. (G) Immunoreactive scores (IRSs) were calculated and compared among groups.

activating serum and milk transferrin. The internal pathway is activated by blocking intracellular antioxidant enzymes such as GPX4 [47]. GPX4 uses glutathione (GSH) as a reduction cofactor to reduce lipid hydroperoxides to lipid alcohols. Several studies have shown that ferroptosis plays an important role in tumor suppression [48]. There is growing evidence that drug-resistant cancer cells are particularly sensitive to ferroptosis [48]. Given that cancer cells consume more iron than healthy cells, ferroptosis is not only an excellent alternative to triggering cell

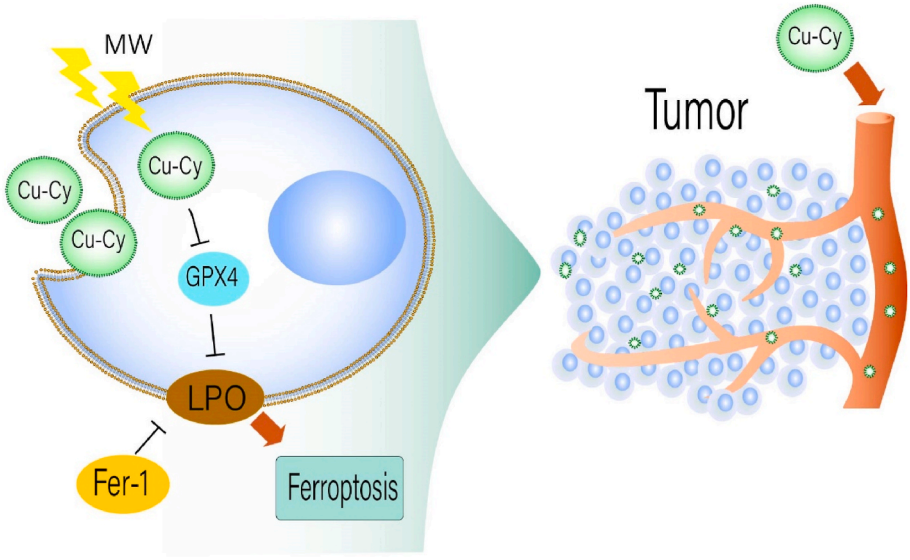

Fig. 6. Schematic illustration of Cu-Cy mediated microwave dynamic therapy (MWDT) for colorectal cancer treatment by inducing cell ferroptosis.

death and reversing drug resistance, but also offers therapeutic selectivity. Radiotherapy can induce ferroptosis, and ferroptosis plays an important role in cell death and tumor suppression induced by radiotherapy [48]. In addition, the synergistic effect of ferroptosis and apoptosis is expected to overcome tumor apoptosis resistance and multidrug resistance, providing a new therapeutic strategy for chemotherapy-resistant tumors [49]. We detected GPX4, one of the markers of ferroptosis, and observed the decrease of GPX4 expression in cells treated with MWDT. Furthermore, MDA and LPO levels were significantly increased after MWDT. Moreover, the addition of ferroptosis inhibitor promoted the expression of GPX4 and decreased the content of MDA and LPO. We also found that the expression level of GPX4 in MWDT group was significantly lower than that in other groups. The data suggests that MW activated Cu-Cy may induce ferroptosis *in vivo* and *in vitro* as illustrated in Fig. 6.

In this study, we found that MW-activated Cu-Cy triggered ferroptosis in HCT15 cells, providing a new idea for further understanding the mechanism of MWDT in cancer treatment. Ferroptosis can affect the efficacy of chemotherapy, radiotherapy, and immunotherapy [50]. Therefore, Cu-Cy mediated MWDT may be combined with chemotherapy, radiotherapy, and immunotherapy to improve the efficacy of these treatments. In addition, cancer cells may have particular susceptibility to ferroptosis when they have a high likelihood to metastasize, or they are resistant to conventional therapeutics, so MWDT may be able to target these cancer cells. Inducing ferroptosis may be an effective treatment strategy to prevent the development of acquired resistance to a variety of drugs, including lapatinib, erlotinib, trametinib, dabrafenib, and vemurafenib [51,52]. Some resistant tumor cells showed signs of EMT (up-regulation of stromal markers and down-regulation of epithelial markers) and, as a result, they became sensitive to ferroptosis [20]. Cu-Cy mediated MWDT could also serve as a new therapeutic tool for drug-resistant tumor cells.

Copper is an essential cofactor for all organisms, and yet it becomes toxic at higher concentrations. The cause of cell death due to excess copper is not clearly understood yet. This is likely related to the ROS production by the Fenton-like reaction induced by copper ions (Cu^{+}, Cu^{2+}) [53]. The Fenton reaction has been extensively explored for cancer treatment [53,54]. We reported Cu-Cy NPs can cause tumor cell death without any external activation, which is attributed to their Fenton-like effect [10]. Recently, it has been reported that copper can induce cell death by targeting lipoylated tricarboxylic acid (TCA) proteins [55]. We believe that these new copper-based properties can be incorporated in our nanoparticle platform for effective cancer treatment and overcome the potential issue of excess copper toxicity to other tissues and cells. Cu-Cy mediated MWDT will be a promising method for tumor treatment as illustrated in Fig. 6.

Also, we need to point out that the temperature generated by 20W microwave irradiation for 3 min was not high enough to kill the tumor cells, and the morphology and vitality of cells were not significantly changed by microwave treatment alone. Therefore, the thermal effect generated by microwave was not the main role in destroying cancer cells. However, the microwave heating is helpful for blood flowing with possible oxygenation which is beneficial for ROS formation and PDT efficiency.

5. Conclusions

In summary, for the first time, we report microwave-induced Cu-Cy-based PDT as a promising cancer treatment to overcome cancer resistance in combination with ferroptosis. Cu-Cy can effectively destroy HCT15 CRC cells with average IC-50 values of 20 μg/mL upon MW irradiation. The cytotoxicity of Cu-Cy to tumor cells after MW stimulation can be alleviated by ferroptosis inhibitor. Furthermore, Cu-Cy mediated MWDT could deplete GPX4 and enhance LPO MDA. The superior *in vivo* antitumor efficacy of the Cu-Cy was corroborated by a HCT15 tumor-bearing mice model. Immunohistochemical experiments showed that the GPX4 expression level in Cu-Cy + MW group was significantly lower than that in other groups. In this study, a novel photosensitizer Cu-Cy was combined with microwave to induce ferroptosis for tumor treatment. Interestingly, induction of ferroptosis suggests that our method could be applied to a wide range of tumor cells that are resistant to other treatments.

Ethic agreement and compliance

The authors declare that they will follow the ethics for authorship, review and the authentic for the research and data.

CRediT authorship contribution statement

Hui Zhou: Methodology, Synthesis, Cell Studies, and Characterization. **Zhongtao Liu:** Methodology, Synthesis, Cell Studies, and Characterization. **Zijian Zhang:** Methodology, Synthesis, Cell Studies, and Characterization. **Nil Kanatha Pandey:** Methodology, Synthesis, Cell Studies, and Characterization. **Eric Amador:** Methodology, Synthesis, Cell Studies, and Characterization, Formal analysis, editing. **William Nguyen:** Formal analysis, editing. **Lalit Chudal:** Formal analysis, editing. **Li Xiong:** Conceptualization, Instruction, Funding acquisition, and Writing. **Wei Chen:** Conceptualization, Instruction, Funding acquisition, and Writing, Visualization, Validation, Supervision. **Yu Wen:** Conceptualization, Instruction, Funding acquisition, and Writing, Visualization, Validation, Supervision.

Acknowledgement

We are grateful for the support by the Natural Science Foundation of China (81773293, 81873640, 81970569, 82000756), Natural Science Foundation of Hunan Province, No.2022JJ40700, the Key Project of Science and Technology Program of Hunan Provincial Science and Technology Department (2015GK3117, 2017WK2063). We would like to acknowledge the supports from Guangxi Jialouyuan Medical Inc., Solgro, and the distinguished award from UT Arlington as well as ROSFORCURE Inc.

References

[1] S. Srivastava, E.J. Koay, A.D. Borowsky, A.M. De Marzo, S. Ghosh, P.D. Wagner, B. S. Kramer, Cancer overdiagnosis: a biological challenge and clinical dilemma, Nat. Rev. Cancer 19 (6) (2019) 349–358.
[2] R.J. DeBerardinis, Tumor microenvironment, metabolism, and immunotherapy, N. Engl. J. Med. 382 (9) (2020) 869–871.
[3] G. Petroni, A. Buqué, L.M. Coussens, L. Galluzzi, Targeting oncogene and non-oncogene addiction to inflame the tumour microenvironment, Nat. Rev. Drug Discov. 21 (6) (2022) 440–462.
[4] V. Bhandari, C. Hoey, L.Y. Liu, E. Lalonde, J. Ray, J. Livingstone, R. Lesurf, Y. J. Shiah, T. Vujcic, X. Huang, S.M.G. Espiritu, L.E. Heisler, F. Yousif, V. Huang, T. N. Yamaguchi, C.Q. Yao, V.Y. Sabelnykova, M. Fraser, M.L.K. Chua, T. van der Kwast, S.K. Liu, P.C. Boutros, R.G. Bristow, Molecular landmarks of tumor hypoxia across cancer types, Nat. Genet. 51 (2) (2019) 308–318.
[5] Y. Wan, L.H. Fu, C. Li, J. Lin, P. Huang, Conquering the hypoxia limitation for photodynamic therapy, Adv. Mater. 33 (48) (2021), e2103978.
[6] M. Li, F. Zhang, Y. Su, J. Zhou, W. Wang, Nanoparticles designed to regulate tumor microenvironment for cancer therapy, Life Sci. 201 (2018) 37–44.
[7] Y. Zhao, S. Wang, Y. Ding, Z. Zhang, T. Huang, Y. Zhang, X. Wan, Z.L. Wang, L. Li, Piezotronic effect-augmented Cu(2-x)O-BaTiO(3) sonosensitizers for multifunctional cancer dynamic therapy, ACS Nano 16 (6) (2022) 9304–9316.
[8] Y. Liu, J. Wu, Y. Jin, W. Zhen, Y. Wang, J. Liu, L. Jin, S. Zhang, Y. Zhao, S. Song, Y. Yang, H. Zhang, Copper(I) phosphide nanocrystals for in situ self-generation magnetic resonance imaging-guided photothermal-enhanced chemodynamic synergetic therapy resisting deep-seated tumor, Adv. Funct. Mater. 29 (2019), 1904678.
[9] T. Gu, H. Dong, T. Lu, L. Han, Y. Zhan, Fluoride ion accelerating degradation of organic pollutants by Cu(II)-catalyzed Fenton-like reaction at wide pH range, J. Hazard Mater. 377 (2019) 365–370.
[10] L. Chudal, N.K. Pandey, J. Phan, O. Johnson, W. Chen, Copper-cysteamine nanoparticles as a heterogeneous fenton-like catalyst for highly selective cancer treatment, ACS Appl. Bio Mater. 3 (3) (2020) 1804–1814.
[11] G. Zhang, W. Xie, Z. Xu, Y. Si, Q. Li, X. Qi, Y. Gan, Z. Wu, G. Tian, CuO dot-decorated Cu@Gd(2)O(3) core-shell hierarchical structure for Cu(i) self-supplying

chemodynamic therapy in combination with MRI-guided photothermal synergistic therapy, Mater. Horiz. 8 (3) (2021) 1017–1028.
[12] S. Kwiatkowski, B. Knap, D. Przystupski, J. Saczko, E. Kędzierska, K. Knap-Czop, J. Kotlińska, O. Michel, K. Kotowski, J. Kulbacka, Photodynamic therapy - mechanisms, photosensitizers and combinations, Biomed. Pharmacother. 106 (2018) 1098–1107.
[13] M. Huo, L. Wang, L. Zhang, C. Wei, Y. Chen, J. Shi, Photosynthetic tumor oxygenation by photosensitizer-containing cyanobacteria for enhanced photodynamic therapy, Angew Chem. Int. Ed. Engl. 59 (5) (2020) 1906–1913.
[14] W.J. Zhi, L.F. Wang, X.J. Hu, Recent advances in the effects of microwave radiation on brains, Mil Med Res 4 (1) (2017) 29.
[15] D. Long, T. Liu, L. Tan, H. Shi, P. Liang, S. Tang, Q. Wu, J. Yu, J. Dou, X. Meng, Multisynergistic platform for tumor therapy by mild microwave irradiation-activated chemotherapy and enhanced ablation, ACS Nano 10 (10) (2016) 9516–9528.
[16] N.K. Pandey, W. Xiong, L. Wang, W. Chen, B. Bui, J. Yang, E. Amador, M. Chen, C. Xing, A.A. Athavale, Y. Hao, W. Feizi, L. Lumata, Aggregation-induced emission luminogens for highly effective microwave dynamic therapy, Bioact. Mater. 7 (2022) 112–125.
[17] X. Ma, X. Ren, X. Guo, C. Fu, Q. Wu, L. Tan, H. Li, W. Zhang, X. Chen, H. Zhong, X. Meng, Multifunctional iron-based Metal-Organic framework as biodegradable nanozyme for microwave enhancing dynamic therapy, Biomaterials 214 (2019), 119223.
[18] C. Fu, H. Zhou, L. Tan, Z. Huang, Q. Wu, X. Ren, J. Ren, X. Meng, Microwave-activated Mn-doped zirconium metal-organic framework nanocubes for highly effective combination of microwave dynamic and thermal therapies against cancer, ACS Nano 12 (3) (2018) 2201–2210.
[19] Q. Wu, N. Xia, D. Long, L. Tan, W. Rao, J. Yu, C. Fu, X. Ren, H. Li, L. Gou, P. Liang, J. Ren, L. Li, X. Meng, Dual-functional supernanoparticles with microwave dynamic therapy and microwave thermal therapy, Nano Lett. 19 (8) (2019) 5277–5286.
[20] J.P. Friedmann Angeli, D.V. Krysko, M. Conrad, Ferroptosis at the crossroads of cancer-acquired drug resistance and immune evasion, Nat. Rev. Cancer 19 (7) (2019) 405–414.
[21] B.R. Stockwell, Ferroptosis turns 10: emerging mechanisms, physiological functions, and therapeutic applications, Cell 185 (14) (2022) 2401–2421.
[22] J. Garcia-Bermudez, K. Birsoy, A mitochondrial gatekeeper that helps cells escape death by ferroptosis, Nature 593 (7860) (2021) 514–515.
[23] C. Zhang, X. Liu, S. Jin, Y. Chen, R. Guo, Ferroptosis in cancer therapy: a novel approach to reversing drug resistance, Mol. Cancer 21 (1) (2022) 47.
[24] T.C. Chen, J.Y. Chuang, C.Y. Ko, T.J. Kao, P.Y. Yang, C.H. Yu, M.S. Liu, S.L. Hu, Y. T. Tsai, H. Chan, W.C. Chang, T.I. Hsu, AR ubiquitination induced by the curcumin analog suppresses growth of temozolomide-resistant glioblastoma through disrupting GPX4-Mediated redox homeostasis, Redox Biol. 30 (2020), 101413.
[25] T. Hong, G. Lei, X. Chen, H. Li, X. Zhang, N. Wu, Y. Zhao, Y. Zhang, J. Wang, PARP inhibition promotes ferroptosis via repressing SLC7A11 and synergizes with ferroptosis inducers in BRCA-proficient ovarian cancer, Redox Biol. 42 (2021), 101928.
[26] Z. Jiang, S.O. Lim, M. Yan, J.L. Hsu, J. Yao, Y. Wei, S.S. Chang, H. Yamaguchi, H. H. Lee, B. Ke, J.M. Hsu, L.C. Chan, G.N. Hortobagyi, L. Yang, C. Lin, D. Yu, M. C. Hung, TYRO3 induces anti-PD-1/PD-L1 therapy resistance by limiting innate immunity and tumoral ferroptosis, J. Clin. Invest. 131 (8) (2021).
[27] M. Alias, N.D. Alkhaldi, M. Reguero, L. Ma, J. Zhang, C. de Graaf, M.N. Huda, W. Chen, Theoretical studies on the energy structures and optical properties of copper cysteamine - a novel sensitizer, Phys. Chem. Chem. Phys. 21 (37) (2019) 21084–21093.
[28] L. Ma, W. Chen, G. Schatte, W. Wang, A.G. Joly, Y. Huang, R. Sammynaiken, M. Hossu, A new Cu–cysteamine complex: structure and optical properties, J. Mater. Chem. C 2 (21) (2014) 4239–4246.
[29] X. Zhen, L. Chudal, N.K. Pandey, J. Phan, X. Ran, E. Amador, X. Huang, O. Johnson, Y. Ran, W. Chen, M.R. Hamblin, L. Huang, A powerful combination of copper-cysteamine nanoparticles with potassium iodide for bacterial destruction, Mater Sci Eng C Mater Biol Appl 110 (2020), 110659.
[30] X. Zhen, N.K. Pandey, E. Amador, W. Hu, B. Liu, W. Nong, W. Chen, Liyi Huang, Potassium iodide enhances the anti-hepatocellular carcinoma effect of copper-cysteamine nanoparticle mediated photodynamic therapy on cancer treatment, Materials Today Physics 27 (2022), 100838.
[31] P. Wang, X. Wang, L. Ma, S. Sahi, L. Li, X. Wang, Q. Wang, Y. Chen, W. Chen, Q. Liu, Nanosonosensitization by using copper–cysteamine nanoparticles augmented sonodynamic cancer treatment, part. Part, Syst. Charact. 35 (4) (2018), 1700378, 1-10.
[32] Z. Liu, L. Xiong, G. Ouyang, L. Ma, S. Sahi, K. Wang, L. Lin, H. Huang, X. Miao, W. Chen, Y. Wen, Investigation of copper cysteamine nanoparticles as a new type of radiosensitiers for colorectal carcinoma treatment, Sci. Rep. 7 (1) (2017) 9290.
[33] Q. Zhang, X. Guo, Y. Cheng, L. Chudal, N.K. Pandey, J. Zhang, L. Ma, Q. Xi, G. Yang, Y. Chen, X. Ran, C. Wang, J. Zhao, Y. Li, L. Liu, Z. Yao, W. Chen, Y. Ran, R. Zhang, Use of copper-cysteamine nanoparticles to simultaneously enable radiotherapy, oxidative therapy and immunotherapy for melanoma treatment, Signal Transduct. Targeted Ther. 5 (1) (2020) 58.
[34] X. Chen, J. Liu, Y. Li, N.K. Pandey, T. Chen, L. Wang, E.H. Amador, W. Chen, F. Liu, E. Xiao, W. Chen, Study of copper-cysteamine based X-ray induced photodynamic therapy and its effects on cancer cell proliferation and migration in a clinical mimic setting, Bioact. Mater. 7 (2022) 504–514.
[35] N.K. Pandey, L. Chudal, J. Phan, L. Lin, O. Johnson, M. Xing, J.P. Liu, H. Li, X. Huang, Y. Shu, W. Chen, A facile method for the synthesis of copper-cysteamine nanoparticles and study of ROS production for cancer treatment, J. Mater. Chem. B 7 (42) (2019) 6630–6642.
[36] M. Yao, L. Ma, L. Li, J. Zhang, R. Lim, W. Chen, Y. Zhang, A new modality for cancer treatment–nanoparticle mediated microwave induced photodynamic therapy, J. Biomed. Nanotechnol. 12 (10) (2016) 1835–1851.
[37] Y. Chang, F. Wu, N.K. Pandey, L. Chudal, M. Xing, X. Zhang, L. Nguyen, X. Liu, J. P. Liu, W. Chen, Z. Pan, Combination of disulfiram and copper-cysteamine nanoparticles for an enhanced antitumor effect on esophageal cancer, ACS Appl. Bio Mater. 3 (10) (2020) 7147–7157.
[38] X. Chu, K. Li, H. Guo, H. Zheng, S. Shuda, X. Wang, J. Zhang, W. Chen, Y. Zhang, Exploration of graphitic-C3N4 quantum dots for microwave-induced photodynamic therapy, ACS Biomater. Sci. Eng. 3 (2017) 1836–1844.
[39] X. Chu, L. Mao, O. Johnson, K. Li, J. Phan, Q. Yin, L. Li, J. Zhang, **W. Chen**, Y. Zhang, Exploration of TiO_2 Nanoparticle Mediated Microdynamic Therapy on Cancer Treatment, Nanomedicine NBM , 18 (2019) 272–281.
[40] P. Wang, X. Wang, L. Ma, S. Sahi, L. Li, X. Wang, Q. Wang, Y. Chen, **W. Chen**, and Q. Liu, Nanosonosensitization by using Copper-Cysteamine Nanoparticles Augmented Sonodynamic Cancer Treatment, Part. Part. Syst. Charact. (2018) 1700378.
[41] T. Wu, X. Liang, X. Liu, Y. Li, Y. Wang, L. Kong, M. Tang, Induction of ferroptosis in response to graphene quantum dots through mitochondrial oxidative stress in microglia, Part. Fibre Toxicol. 17 (1) (2020) 30.
[42] E. Dekker, P.J. Tanis, J.L.A. Vleugels, P.M. Kasi, M.B. Wallace, Colorectal cancer, Lancet 394 (10207) (2019) 1467–1480.
[43] H. Zhou, Z. Liu, Y. Wang, X. Wen, E.H. Amador, L. Yuan, X. Ran, L. Xiong, Y. Ran, W. Chen, Y. Wen, Colorectal liver metastasis: molecular mechanism and interventional therapy, Signal Transduct. Targeted Ther. 7 (1) (2022) 70.
[44] X. Chen, J. Li, R. Kang, D.J. Klionsky, D. Tang, Ferroptosis: machinery and regulation, Autophagy 17 (9) (2021) 2054–2081.
[45] Y. Kinowaki, T. Taguchi, I. Onishi, S. Kirimura, M. Kitagawa, K. Yamamoto, Overview of ferroptosis and synthetic lethality strategies, Int. J. Mol. Sci. 22 (17) (2021) 9271.
[46] X. Chen, R. Kang, G. Kroemer, D. Tang, Broadening horizons: the role of ferroptosis in cancer, Nat. Rev. Clin. Oncol. 18 (5) (2021) 280–296.
[47] M.R. Valashedi, N. Najafi-Ghalehlou, A. Nikoo, C. Bamshad, K. Tomita, Y. Kuwahara, T. Sato, A.M. Roushandeh, M.H. Roudkenar, Cashing in on ferroptosis against tumor cells: usher in the next chapter, Life Sci. 285 (2021), 119958.
[48] E. Ozkan, F. Bakar-Ates, Ferroptosis: a trusted ally in combating drug resistance in cancer, Curr. Med. Chem. 29 (1) (2022) 41–55.
[49] J. Fu, T. Li, Y. Yang, L. Jiang, W. Wang, L. Fu, Y. Zhu, Y. Hao, Activatable nanomedicine for overcoming hypoxia-induced resistance to chemotherapy and inhibiting tumor growth by inducing collaborative apoptosis and ferroptosis in solid tumors, Biomaterials 268 (2021), 120537.
[50] Y. Mou, J. Wang, J. Wu, D. He, C. Zhang, C. Duan, B. Li, Ferroptosis, a new form of cell death: opportunities and challenges in cancer, J. Hematol. Oncol. 12 (1) (2019) 34.
[51] B. Hassannia, P. Vandenabeele, T. Vanden Berghe, Targeting ferroptosis to iron out cancer, Cancer Cell 35 (6) (2019) 830–849.
[52] G.Q. Chen, F.A. Benthani, J. Wu, D. Liang, Z.X. Bian, X. Jiang, Artemisinin compounds sensitize cancer cells to ferroptosis by regulating iron homeostasis, Cell Death Differ. 27 (1) (2020) 242–254.
[53] X. Meng, X. Zhang, M. Liu, B. Cai, N. He, Z. Wang, Fenton reaction-based nanomedicine in cancer chemodynamic and synergistic therapy, Appl. Mater. Today 21 (2020), 100864.
[54] S. Xiao, Y. Lu, M. Feng, M. Dong, Z. Cao, X. Zhang, Y. Chen, J. Liu, Multifunctional FeS_2 theranostic nanoparticles for photothermal-enhanced chemodynamic/photodynamic cancer therapy and photoacoustic imaging, Chem. Eng. J. 396 (2020), 125294.
[55] P. Tsvetkov, S. Coy, B. Petrova, M. Dreishpoon, A. Verma, M. Abdusamad, J. Rossen, L. Joesch-Cohen, R. Humeidi, R.D. Spangler, J.K. Eaton, E. Frenkel, M. Kocak, S.M. Corsello, S. Lutsenko, N. Kanarek, S. Santagata, T.R. Golub, Copper induces cell death by targeting lipoylated TCA cycle proteins, Science 375 (2022) 1254–1261.